

Control and Application of Beam Microbunching in High Brightness Linac-driven Free Electron Lasers

Gennady Stupakov

SLAC National Accelerator Laboratory, Menlo Park, CA 94025

5th International Particle Accelerator Conference
Dresden, Germany, June 15 - 20, 2014

Microbunching instability workshops

Microbunching instability workshops:

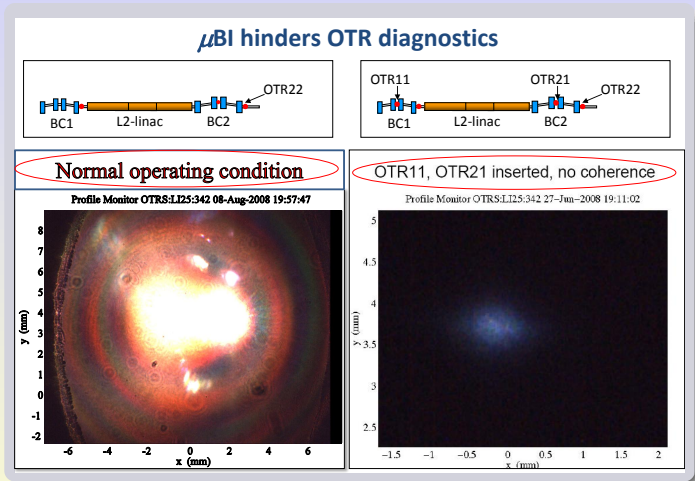
- 1st Microbunching Instability Workshop, September 17-19, 2007, (Trieste, Italy).
- 2nd Microbunching Instability Workshop, Oct. 6-8, 2008, (LBNL, USA)
- 3d Microbunching Instability Workshop, March 24-26, 2010, (Frascati, Italy).
- 4th Microbunching Instability Workshop, April 11-13, 2012, (College Park, MD, USA).
- 5th Microbunching Instability Workshop, 8 - 10 May 2013, (Pohang Accelerator Laboratory, Korea).
- 6th Microbunching Instability Workshop, 6 - 8 October 2014, (Trieste, Italy).

Outline of the talk

- Introduction
- Mechanism of microbunching instability (MBI)
- Wakefields causing microbunching
- Microbunching in a bunch compressor
- Laser heater
- Suppressing MBI without the laser heater
- Using MBI for generation of UV radiation
- Noise suppression—an example of “anti-microbunching”
- Summary

Microbunched beam at LCLS BC2

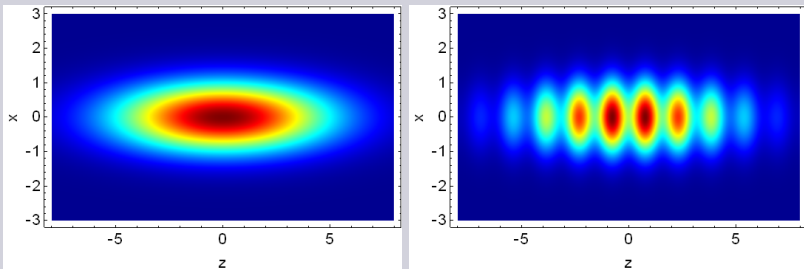
Image of microbunched beam at LCLS.



Courtesy H. Loos

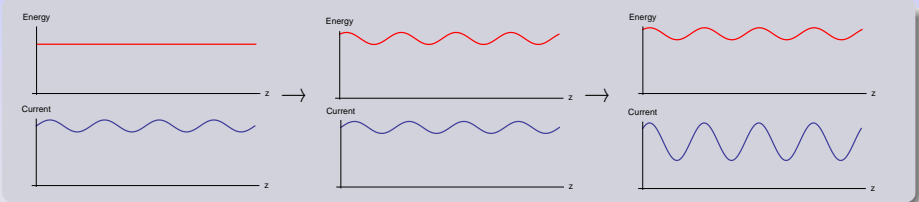
Microbunching means short wavelengths

Microbunching in linear accelerators has a typical wavelength of the modulation much shorter than the bunch length.



Instability is excited by the wake fields in the machine in combination with energy dependent longitudinal displacements.

Mechanism of MBI

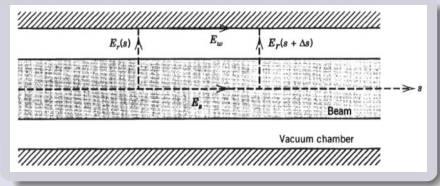


- Initial density perturbation in the beam due to shot noise
- Due to the wake ΔI induces energy modulation in the beam, $\Delta E = eZ \times \Delta I$
- Slippage that depends on energy translates ΔE into $\Delta n \rightarrow \Delta I$. Under certain conditions, the final ΔI is greater than the initial one.

Mechanism of MBI

- The slippage can be provided by velocity dependence versus energy. For ultra-relativistic beams $v_z \approx c$, and the slippage is dominated by bunch compressors. It is described by R_{56} element of the transport matrix.
- It is believed that MBI starts from shot noise in the beam. It is possible that an RF photo gun can imprint some initial density modulation. MBI was identified in thermionic cathode DC gun at SACLAC and SCSS accelerators in Japan.
- Two dominant wakefields that drive MBI are the longitudinal space charge (LSC) and the wake due to coherent synchrotron radiation (CSR) in bends of bunch compressors.

Longitudinal space charge impedance



A beam of radius a propagates inside a pipe of radius r_w with conducting walls, $a \ll r_w$. For $k \ll \gamma/r_w$,

$$Z_{LSC} \approx i \frac{Z_0 c}{4\pi} \frac{k}{\gamma^2} \left(1 + 2 \ln \frac{r_w}{a} \right)$$

For $\gamma/a \gg k \gg \gamma/r_w$,

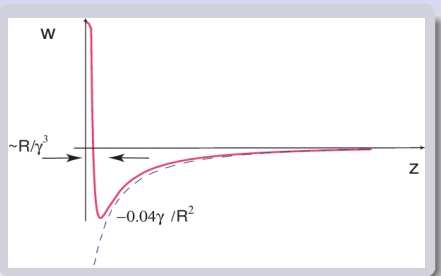
$$Z_{LSC} \approx i \frac{Z_0 c}{4\pi} \frac{k}{\gamma^2} \left(1 + 2 \ln \frac{\gamma}{ak} \right)$$

In the limit $k \gg \gamma/a$ the concept of impedance breaks down—it is only valid if the induced field does not change much through the beam cross section¹. Numerical example: for $a = 100 \mu\text{m}$, $\gamma = 500$ the condition $k \lesssim \gamma/a$ is satisfied for $\lambda \gtrsim 1 \mu\text{m}$.

¹ Venturini, PRST-AB **11**, 034401, (2008); Marinelli, Rosenzweig, PRST-AB **13**, 110703 (2010)

CSR wake—1D steady state

A relativistic particle moving in vacuum in a circular orbit of radius R , in steady state, generates a CSR wake² (per unit length of path).



The wake is localized in front of the particle, $z > 0$.
For $z \ll R$ and $z \gg R/\gamma^3$,

$$w_{\text{CSR}}(z) \approx -\frac{E_{||}}{e} = -\frac{2}{3^{4/3} R^{2/3} z^{4/3}}$$

Area under $w(z)$ is zero.

Longitudinal CSR impedance

$$Z_{\text{CSR}}(k) = \frac{1}{c} \int_0^\infty dz w(z) e^{-ikz} = \frac{Z_0}{4\pi} \frac{2}{3^{1/3}} \Gamma\left(\frac{2}{3}\right) e^{i\pi/6} \frac{k^{1/3}}{R^{2/3}}.$$

² logansen and Rabinovich, JETP, **37**, 83, (1960); Murphy, Krinsky and Gluckstern, PAC (1995); Derbenev et al., TESLA-FEL 95-05, (1995).

Approximations made in 1D steady state CSR wake

Approximations:

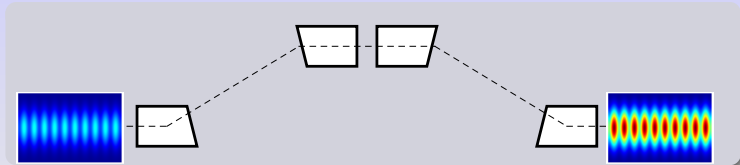
- Metallic walls are far enough from the orbit—the shielding effect is neglected
- Transverse beam size: $\sigma_{\perp} \lesssim l_{\perp} \ll (\lambda^2 R)^{1/3}$ (here $\lambda = 1/k$).
- Transient effects at the entrance to and exit from the magnet are neglected:

$$l_{\text{magnet}} > l_f \sim (\lambda R^2)^{1/3}$$

Geometric impedance is not so important for MBI because it (typically) saturates at large k .

MBI in bunch compressors

Theory of MBI in bunch compressors was developed in 2001-2002³.



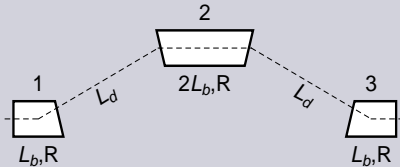
Assume an initial modulation of the beam $n(z) = n_0 + n_i \sin k_i z$. In linear regime, after passage through the chicane, $n(z) = n_0 + n_f \sin k_f z$ with $k_f/k_i = C$ —the compression factor. The gain, or amplification factor

$$G(k_i) = \frac{n_f}{n_i}$$

³ Borland PRST-AB 4, 070701(2001); Heifets, Stupakov and Krinsky, PRST-AB 5, 064401 (2002); Saldin, Schneidmiller and Yurkov, NIM A490, 1 (2002); Huang and Kim, PRST-AB 5, 074401 (2002).

"Klystron instability" model

"Klystron instability" is a simple model⁴ for the calculation of the gain factor G . It assumes the CSR impedance in the magnets and a cold beam.



Take an initial current perturbation $I = I_0 + I_1 \cos kz$ with $I_1 \ll I_0$. After passage through the first magnet the energy modulation in the beam is $\Delta E = eV = eL_b Z_{CSR}(ck)I_1$.

Propagation from 1 to 2 shifts the particles by $\Delta z = (\Delta E/E)R_{56}(1 \rightarrow 2)$, which induces the density perturbation $I_2 = k\Delta z I_0$ (from continuity eq.). Assume $I_2 \gg I_1$ and neglect I_1 . After passage through 2 the energy modulation is $\Delta E = eV = 2L_b e Z_{CSR}(\omega)I_2$. Propagation from 2 to 3 shifts the particles by $\Delta z = (\Delta E/E)R_{56}(2 \rightarrow 3)$, which induces the density perturbation $I_3 = k\Delta z I_0$. Assume $I_3 \gg I_2$ and neglect I_2 . The gain factor $G = I_3/I_1$:

$$G = \frac{2\Gamma^2(2/3)}{3^{5/3}} \frac{I_0}{\gamma I_A} \frac{k^{8/3} |R_{56}^{(ch)}|^2 L_d^2}{R^{4/3}}$$

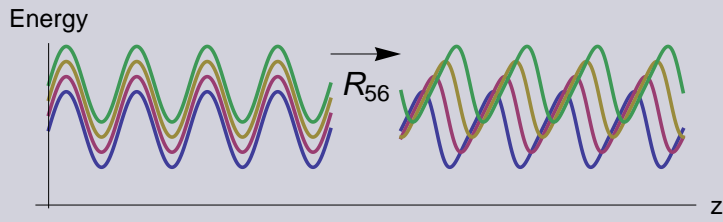
For a cold beam G increases with k .

⁴Saldin, Schneidmiller and Yurkov, NIMA 490, 1, (2002).

Effect of energy spread on MBI

More sophisticated models involve solution of the Vlasov equation for the evolution of the distribution function through the system. They take into account the energy spread, finite emittance and compression effect (energy chirp).

They predict that σ_E and ϵ tend to suppress G (Landau damping).



Smearing of microbunching occurs if

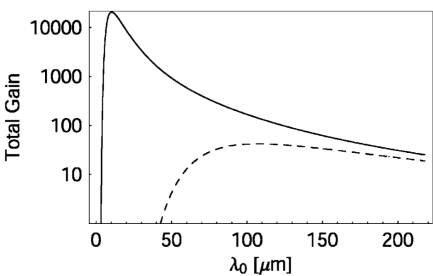
$$R_{56} \frac{\sigma_E}{E} \gtrsim \lambda$$

Energy spread and emittance

Effect of compression, energy spread and finite emittance add to the gain the factor

$$e^{-C^2 k^2 (\sigma_E/E)^2 R_{56}^2/2} \times e^{-C^2 k^2 (\epsilon/2\beta)(\beta^2 R_{51}^2 + R_{52}^2)}$$

Example of the gain calculation for LCLS, $\sigma_E \sim 3$ keV

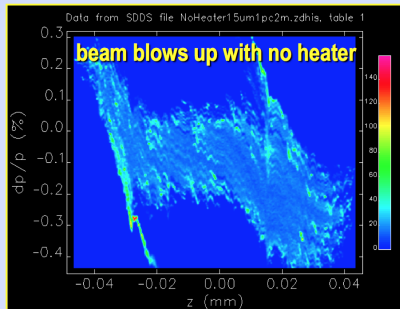
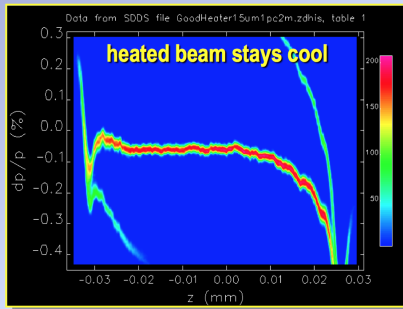


MBI gain calculated for LCLS as a function of the initial modulation wavelength λ_0 with $\sigma_E \sim 3$ keV (solid curve) and the energy spread increased by about a factor of 10 (dashed curve) (from Z. Huang, et al., PRST-AB 7, 074401 (2004)).

Increasing energy spread suppresses the instability

The slice energy spread of the beam can be set to the level which, on the one hand, suppresses development of the microbunching instability, but, at the same time, is small enough to not impede lasing in the FEL.

Final long. phase space at 14 GeV for initial modulation of 1% at $\lambda = 15 \mu\text{m}$

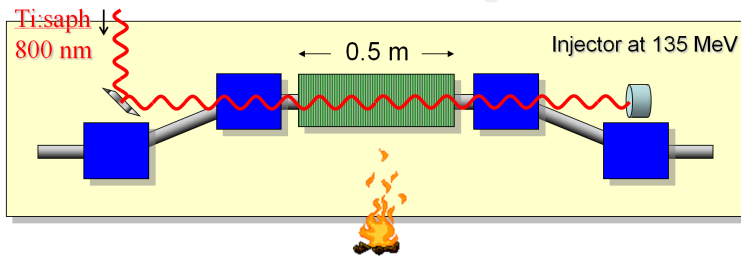


Courtesy P. Emma

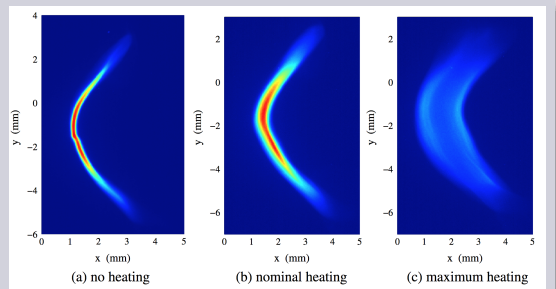
Increasing energy spread suppresses the instability

The laser heater was proposed by Saldin, Schneidmiller and Yurkov (2004). It is now considered as a necessary attribute in practically all designs of modern x-ray FELs.

Laser heater design



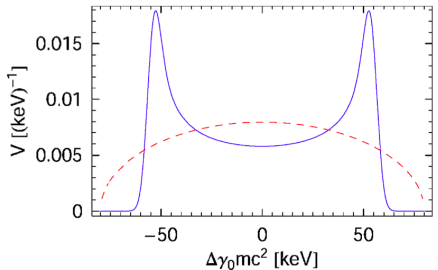
Measurement of energy spread induced by LH at LCLS



Measured longitudinal phase space at 135 MeV with (a) laser heater off, (b) IR-laser energy at $10 \mu\text{J}$, and (c) at $220 \mu\text{J}$. The vertical axis shows beam longitudinal position and the horizontal axis shows the beam energy (from⁵).

⁵Z. Huang, et al., PRST-AB 13, 020703 (2010).

LH is not a “true” heater



The resulting energy distribution function depends on the ratio of $\sigma_{\perp b}$ and laser $\sigma_{\perp L}$. In the limit $\sigma_{\perp L} \gg \sigma_{\perp b}$ one finds a double-horn distribution in energy. In the case when the laser pulse is matched to the beam size, $\sigma_{\perp L} \approx \sigma_{\perp b}$, the distribution function becomes Gaussian-like.

Non-thermal nature of LH appears in the “trickle heating” phenomenon which is due to incomplete smearing of the structures introduced by the laser in the beam at small laser energy⁶. Non-Gaussian electron energy heating has an impact on the performance of a seeded FEL⁷.

⁶ Z. Huang, et al., PRST-AB **13**, 020703 (2010).

⁷ E. Ferrari, et al., PRL **112**, 114802 (2014).

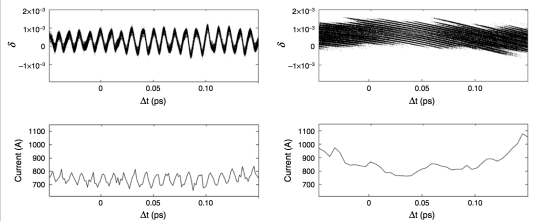
Suppressing MBI without LH

While the laser heater provides a reliable way to fight MBI, it is not completely satisfactory solution. It increases the longitudinal emittance of the beam, which can be critical for seeded FELs.

Several approaches has been proposed in literature to suppress MBI without using LH.

Allow self-heating of the beam through LSC

Idea: accumulate a certain amount of energy modulation via LSC in the linac, remove any residual linear energy chirp in the bunch, and finally “smear out” the longitudinal phase space by means of a strong magnetic chicane⁸.



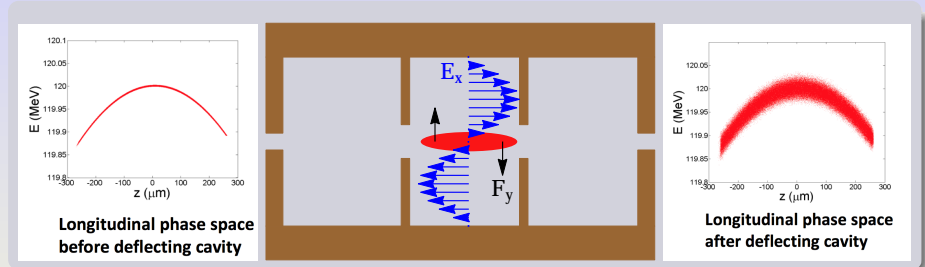
Simulations for FERMI FEL.
Left: longitudinal phase space (top) and current profile (bottom) of the bunch core at the entrance of FERMI BC2. An initial 30 μ m wavelength and 1% amplitude density modulation was imposed to the beam.

Right: longitudinal phase space (top) and current profile (bottom) of the bunch core at the exit of FERMI BC2.

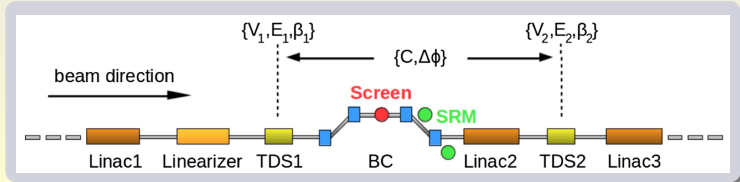
⁸ Di Mitri, et al., PRST-AB **13** 010702 (2010); Di Mitri, Cornacchia, Physics Reports, **539**, 1, (2014)

Reversible heater

Reversible heating of the beam can be achieved with two deflecting RF structure⁹ (TDS). TM₁₀₀ mode is excited in the cavity.

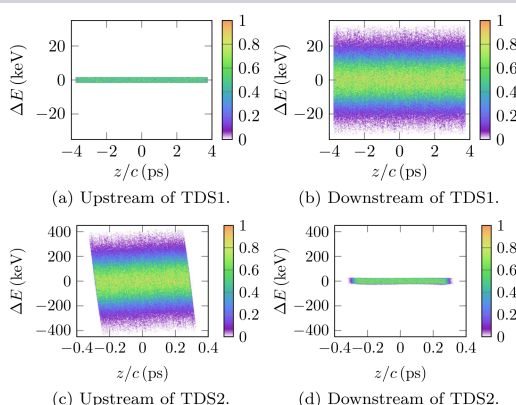


The first structure “heats up” the beam, the second one removes the energy spread.



Reversible heater phase space simulations

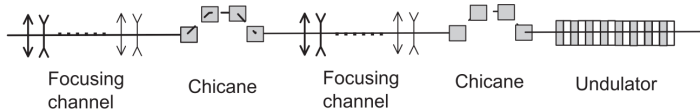
Simulations show the effect of the reversible heater.



Challenging tolerances on the RF phase jitter ($\sigma_\phi \ll 0.012^\circ$) and beam energy jitter ($\sigma_E/E \ll 10^{-5}$).

Using MBI for UV generation

Idea: intentionally submit the beam to a small-scale MBI for generation of vacuum ultraviolet and x-ray radiation in FELs¹⁰

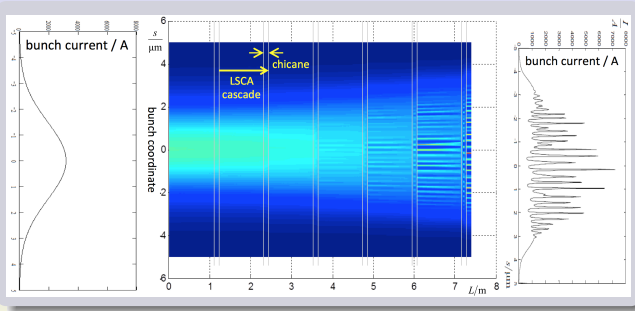


An optimized setup: $E_b = 3 \text{ GeV}$, $I_b = 2 \text{ kA}$, $\epsilon_n = 2 \mu\text{m}$, and $\sigma_E = 0.3 \text{ MeV}$. With the beta function $\beta = 1.4 \text{ m}$ and $R_{56} = 25 \mu\text{m}$ one can achieve the total gain of about $G = 10^3$ in 2-3 stages at the wavelength $\lambda \approx 15 \text{ nm}$. After the last chicane a tunable-gap undulator with the period length of 5 cm and a number of periods 30 is installed. The undulator selects a relatively narrow band of about 3% from the broadband density modulations. The peak power within the central cone is estimated at a gigawatt level.

¹⁰Schneidmiller and Yurkov, PRST-AB **13**, 110701 (2010); M. Dohlus et al., IPAC 2011, 1449 (2011).

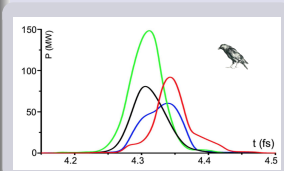
Using MBI for UV generation

In a further development of the idea the authors utilize the broadband nature of the MBI amplification and show how one can achieve attosecond pulses of radiation in this scheme.



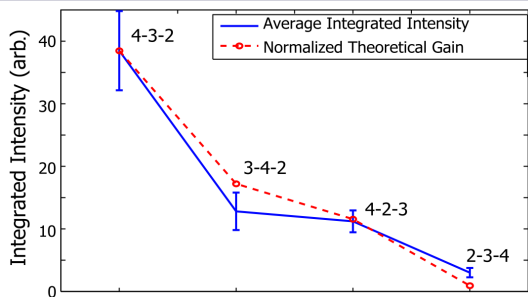
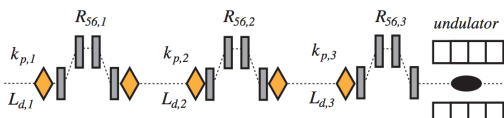
Courtesy M. Dohlus.

Generation of 4.3 nm radiation with multi-stage MBI.



NLCTA experiment at SLAC

Experimental demonstration of a cascaded longitudinal space-charge amplifier at optical wavelengths at NLCTA (SLAC)¹¹.



The on-axis gain is estimated to exceed 4 orders of magnitude

¹¹ A. Marinelli et al., PRL 110, 264802 (2013)

Noise reduction in relativistic beams

Can fluctuations (noise) in electron beam be made smaller than shot noise? The general idea of noise suppression in beams is known from RF sources—after a quarter of plasma oscillations in an electron beam the shot noise is reduced.

Noise suppression in relativistic beams was proposed by Gover and Dyunin¹² and other authors¹³. Possible applications include: suppression of the fundamental harmonic in favor of higher harmonics in FELs; noise suppression for seeding; application in collective electron cooling.

A simple 1D model: cold beam particles interact via Coulomb forces in a straight region and then pass through a chicane. The beam initially is assumed to have shot noise (uncorrelated positions of particles).



¹² PRL, 102, 154801, (2009).

¹³ Litvinenko, FEL2009, p. 229, (2009).; Ratner et al., PRST-AB **14**, 060710 (2011).

Noise reduction in relativistic beams



The 1D formfactor which characterizes noise and determines radiation of the beam after the dispersive section¹⁴

$$F = 1 + N \langle e^{ik(z_1 - z_2)} \rangle = (1 - \gamma)^2$$

with

$$\gamma = n_0 R_{56} \frac{4\pi r_e L_a}{S\gamma}$$

n_0 - number of particles per unit length

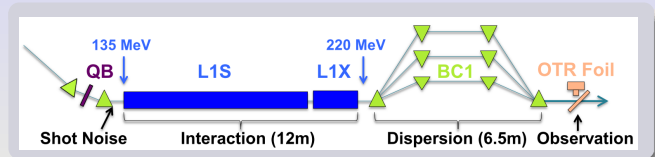
S - beam transverse area

L_a - length of interaction region

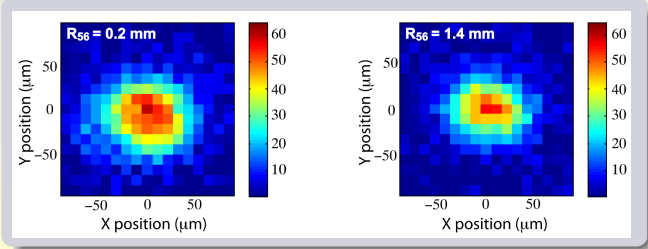
¹⁴ Ratner et al., PRST-AB **14**, 060710 (2011).

Noise suppression and experiment at LCLS

Noise suppression experiment at LCLS¹⁵. Parameters: $E_b = 135 - 220$ MeV, $Q_b = 5 - 20$ pC, $\epsilon_n = 0.2$ μm . The OTR signal was observed after the BC1 chicane (no energy chirp was introduced in the beam). The intensity was measured as a function of R_{56} of the chicane.



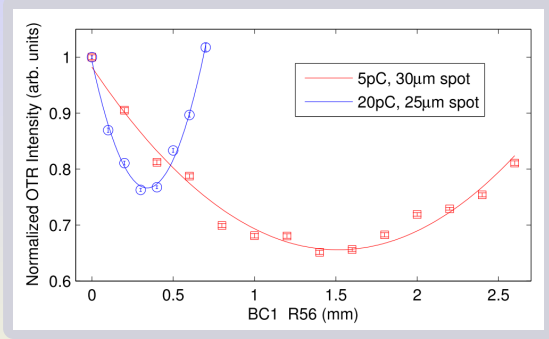
Beam image without noise suppression (left) and with (right).



¹⁵ Ratner, Stupakov, PRL 109, 034801 (2012).

Noise suppression and experiment at LCLS

We expect a quadratic dependence of intensity of OTR versus R_{56} .



From theory we expect the minimal point to be located at $R_{56} \propto 1/Q$. An incomplete suppression is explained by relatively large collection angle of the optics of the CCD camera and finite transverse size of the beam.

Another noise suppression experiment is published by Gover et al.¹⁶

¹⁶ Nature Physics, 8 (12), 877 (2012).

Conclusions

- Beam microbunching is an important part of beam dynamics of modern x-ray FELs that can considerably affect their performance. Modern FEL designs should provide measures to control MBI.
- A well developed theory explains the mechanism behind the microbunching instability: they are driven by CSR and SC wakefields. Computer codes reliably simulate the instability.
- Laser heater is universally employed at existing FELs to suppress MBI (and is planned for future FELs). However, the residual still MBI blinds the OTR diagnostics in the linac. Several promising new ideas were recently proposed to fight the instability; they are still waiting for a convincing experimental demonstration.
- With a proper arrangement, MBI amplified small-scale fluctuations can be used for coherent radiation of vacuum UV and x-rays.
- Noise suppression in relativistic beams is another demonstration of fluctuations control at short wavelengths. It has been studied theoretically in recent years and successfully demonstrated experimentally.